1990

An Acoustic Transfer Matrix Model for Compressor and Condenser Interaction

J. E. Farstad
The Ohio State University

R. Singh
The Ohio State University

AN ACOUSTIC TRANSFER MATRIX MODEL FOR COMPRESSOR AND CONDENSER INTERACTION

Jerry E. Farstad
Graduate Reasearch Associate

and

Rajendra Singh
Professor

Department of Mechanical Engineering
The Ohio State University
206 West 18th Avenue
Columbus, Ohio 43210

ABSTRACT

Previous investigators have used acoustic transfer matrix theory to model discharge pressure pulsations in refrigeration systems. In each of these studies, however, the condenser was treated as an anechoic duct. In this paper, a more realistic acoustic model for the condenser is devevoped which accounts for the effects of system thermal conditions. This is done by constructing a transfer matrix model of variable cross-sectional area from solutions for the steady-state heat transfer in the condenser. Condenser models for two different thermal conditions have been constructed and compared both to each other and to the anechoic condenser model in terms of discharge valve chamber to discharge line acoustic impedance. The effects of these three condenser models on the predicted performance of a discharge line muffler is also examined.

1. INTRODUCTION

Several previous investigators [1-3] have used acoustic transfer matrix theory to model pressure pulsations in refrigeration systems. In each of these studies, the condenser and evaporator were treated as anechoic ducts. Although this approach is mathematically convenient, it may not be adequate for predicting the behavior of real refrigeration systems. This is particularly true when one is interested in predicting the performance of reactive mufflers. Munjal [4], Munjal and Sreenath [5], and Crocker [6] have demonstrated that for internal combustion engines muffler performance is strongly influenced by the acoustic impedances of the source and load between which it is placed. Similar results might be expected for refrigeration systems with reciprocating compressors.

In this paper, the technique developed by others [1-3] is extended. A more realistic acoustic model for a refrigeration condenser which accounts for the effects of thermal conditions is developed using the transfer matrix method. To do this, solutions for the steady-state heat transfer in the condenser are obtained and used to construct a transfer matrix acoustic model of variable cross sectional area. Transfer matrix condenser models have been constructed for two specific sets thermal conditions. The acoustic impedances between the discharge valve chamber and the discharge line have been computed and are compared both to each other and to the results for an anechioc condenser model. This permits study of the acoustic interaction between the compressor and condenser.

2. CONDENSER THERMAL MODEL

The condenser is considered to be a concentric tube heat exchanger, as shown in Figure 1, with refrigerant flowing through the inner tube of diameter d and area S, and cooling water flowing through the annulus. The outer tube is assumed to be well insulated, and the overall heat transfer coefficient between the fluids, U, incorporates convection resistances on both sides of the center tube and the conduction resistance of the tube wall. The refrigerant temperature, T_r, the cooling water temperature, T_w, and the quality of the refrigerant two-phase mixture, X, are assumed to vary only with the axial coordinate, x.

As Figure 1 indicates, the condenser may be considered as having three distinct regions.In the regions near the inlet and outlet, the refrigerant exists entirely as vapor and liquid, respectively. In the center region, it is a two-phase mixture. In either of the single phase regions, T_r and T_w are related by [7]

$$\frac{dT_r}{dx} + \Lambda_r(T_r - T_w) = 0 \tag{1a}$$

$$\frac{dT_w}{dx} + \Lambda_w(T_w - T_r) = 0 \tag{1b}$$

$$\Lambda_r = \frac{\pi dU}{m_r C_r}, \Lambda_w = \frac{\pi dU}{m_w C_w} \tag{1c,1d}$$

Here m_j and C_j are the mass flow rate and specific heat, respectively, of fluid j. Note that U and C_r take on different values in the vapor and liquid single phase regions. The axial coordinate x is a local coordinate with a new origin at the begining of each region. The system (1) is solved subject to initial conditions $T_r(0)=T_{ir}$ and $T_w(0)=T_{iw}$. Solutions are

$$T_r(x) = (T_{ir} - \xi)e^{-(\Lambda_r+\Lambda_w)x} + \xi \tag{2a}$$

$$T_w(x) = (T_{iw} - \xi)e^{-(\Lambda_r+\Lambda_w)x} + \xi \tag{2b}$$

$$\xi = \frac{T_{ir}\Lambda_r + T_{iw}\Lambda_w}{\Lambda_r + \Lambda_w} \tag{2c}$$

The temperature distribution given by (2) is valid to the point where the refrigerant vapor begins to condense. At this point, where T_r reaches the saturation temperature, T_{sat}, the two-phase region begins. Note that T_{sat} is determined by the condenser mean pressure. In this second region, $T_r=T_{sat}$ throughout while the refrigerant quality, X, satisfies [7]

$$\frac{dX}{dx} + \Lambda_{fg}(T_{sat} - T_w) = 0 \tag{3a}$$

$$\Lambda_{fg} = \frac{\pi dU}{m_r h_{fg}} \tag{3b}$$

where h_{fg} is the refrigerant enthalpy of vaporization.

The cooling water temperature T_w again satisfies (1b) in the two-phase region [7]. In (1b) and (3a), however, U is evaluated to account for the new heat transfer conditions in the two-phase region, and the value for Λ_w is recalculated. Equations (3a) and the (1b) are solved subject to initial values X(0)=1 and $T_w(0)=T^*_{iw}$, where T^*_{iw} is the cooling water temperature given by (2b) at the end of the vapor region. Solutions in the two-phase region are

$$X(x) = \frac{\Lambda_{fg}}{\Lambda_w}(T_{sat} - T^*_{iw})(e^{-\Lambda_w x} - 1) + 1 \tag{4a}$$

$$T_w(x) = (T^*_{iw} - T_{sat})e^{-\Lambda_w x} + T_{sat}. \tag{4b}$$

Equation (4a) indicates that for $(\Lambda fg/\Lambda w)(T_{sat} - T^*_{iw})>1$, X will eventually become zero. If the coordinate x where this occurs lies within the finite specified length of the condenser, the two-phase region must end, since negative values of X are not permitted. Beyond this point, the refrigerant exists as a liquid. The fluid temperatures in this region again satisfy (1), with appropriate values of Λr and Λw applied. Solutions given by (2) are again valid, but with T_{ir} and T_{iw} taken as the temperatures at the end of the two-phase region.

Zivi [8] found that for film- type condensation X is related to the part of the tube cross sectional area occupied by vapor, S_g, by

$$\frac{S_g}{S}=\left[1+\left(\frac{1-X}{X}\right)\left(\frac{\rho_g}{\rho_f}\right)^{\frac{2}{3}}\right]^{-1} \tag{5}$$

where S is the total tube area and ρ_g and ρ_f are the densities of the refrigerant vapor and liquid, respectively.

3. CONDENSER ACOUSTIC MODEL

Consider a rigid duct of uniform cross section S and length L which is free of acoustic damping. For such a duct, the acoustic pressure, p ,and the volume velocity, Q, at the ends of the of the duct are related by [9]

$$\begin{Bmatrix} P_1(f) \\ Q_1(f) \end{Bmatrix}=\begin{bmatrix} \cos\frac{2\pi fL}{c} & j\frac{\rho c}{S}\sin\frac{2\pi fL}{c} \\ j\frac{S}{\rho c}\sin\frac{2\pi fL}{c} & \cos\frac{2\pi fL}{c} \end{bmatrix}\begin{Bmatrix} P_2(f) \\ Q_2(f) \end{Bmatrix} \tag{6}$$

where f is the frequency, c is the speed of sound, and j is the imaginary unit. Equation (6) may be used to model the vapor region of the condenser as a duct of area S filled entirely with refrigerant vapor and of length determined from Equation (2) by the value of x when $T_r=T_{sat}$.

Physical property data for refrigerant 12 (CCl_2F_2) indicate that $\rho_f\approx 10\rho_g$ [10] and $c_f\approx 3c_g$ [11]. Hence, the characteristic acoustic impedance of the liquid, $\rho_f c_f$, is approximately thirty times that of the vapor. Because of this, it is reasonable to approximate the the liquid/vapor interface in the two-phase region as an acoustically rigid boundary. This implies that an acoustic wave incident upon the interface is principally reflected back into the vapor rather than propagating through the liquid as previous investigators have assumed [1-3].

These facts may be used to construct an approximate acoustical model for the condenser two-phase region. Although S_g, computed from (4a) and (5), varries continuously with x, it may be approximated by a series of segments of uniform cross section. This results in a stepped-ube model for the two-phase region as shown in Figure 2. The number of steps used and the cross sectional area of each are specified by the analyst such that the approximation to $S_g(x)$ is reasonable. The length of each element is then determined from (4a) and (5). For example, the first element might be chosen to have area $S_g=0.95S$. Its length would be the total axial displacement where $1.0<S_g/S<0.9$. Equation (6) is then applied to each element. The end of the final element is treated as an acoustically rigid boundary, again based on relative properties of the liquid and the vapor.

An acoustic model for the whole condenser is obtained by multiplying together the transfer matricies for the vapor region and each of the elements in the two-phase region. Such a model may be directly substituted for the anechoic discharge line used in compressor and manifold models developed by Singh and Soedel [1]. This permits more realistic simulation of the performance of actual refrigeration systems.

4. EXAMPLE CASES AND RESULTS

To exmine the acoustic interaction between a condenser and a compressor discharge system, stepped-tube transfer matrix models were constructed for the two sets of thermal conditions listed in Table 1. Data for these conditions were obtained experimentally from operation of a system having a water cooled condenser with d=12.7 mm (0.5 in.) [7]. Heat transfer coefficients used to calculate U for each case were estimated from correlations appropriate for the refrigerant and cooling water flows [12]. The data in Table 1 and corresponding values for U were used to compute $S_g(x)$ from equations (2), (4a), and (5) for each thermal condition. These solutions were used to construct stepped-tube condenser models having eleven acoustic elements.The areas of the eleven elements and their lengths for each thermal condition are listed in Table 2.

The transfer matrix model used for the compresor discharge system is illustrated in Figure 3. This model represents a two cylinder compressor discharge system between the valve chambers and discharge line. The stepped-tube condenser models were joined to the discharge system model at element 11 shown in Figure 3. For all of the cases considered, the discharge system model was invariant except for element 10 shown in Figure 3 , which models a discharge line muffler having a length of 117 mm (4.6 in.) and an area expansion ratio of 34. To investigate the effect of thermal conditions on muffler performance, discharge system models with and without mufflers were used with each of the condenser stepped-tube models. The muffler was removed from the model of Figure 3 by setting the area of element 10 equal to that of elements 9 and 11 while its length was unchanged. Discharge system and condenser model pairs were compared by computing the acoustic impedance between one of the valve chambers and a point in the discharge line near the muffler exit, when one was included. These locations correspond to elements 1 and 11 in Figure 3. The valve chamber to discharge line acoustic impedance $Z_{1,11}$ is given by

$$Z_{1,11}(nf_0) = \frac{p_{11}(nf_0)}{Q_1(nf_0)} \tag{7}$$

where n is the harmonic index and f_0 is the compressor shaft speed. For all cases considered, acoustic damping in the refrigerant was neglected and f_0= 57.5 Hz was used.

Results for the two condenser stepped tube models with and without mufflers are shown in Figures 4 and 5, respectively. In these Figures, $Z_{1,11}$ has been computed only at the first ten harmonics of f_0. The points at each harmonic of the resulting line spectra have been joined by straight lines to distinguish the results of one case from those of another. Signifigant differences in the magnitude of $Z_{1,11}$ are observed in Figure 4 when no muffler was included, particularly at the lower frequencies. In fact, for n=2, the impedance magnitude for thermal condition I was approximately 40 dB greater than that for thermal condition II. Because the first few harmonics often dominate $Q_1(nf_0)$ for reciprocating compressors, one might expect the discharge pulsation level for thermal condition I to be 40 dB greater than that for thermal condition II if $Q_1(nf_0)$ were similar for each case. Figure 4 also shows differences in the phase of $Z_{1,11}$ between the two thermal conditions.

When the muffler was included in the discharge system model, Figure 5 shows that the impedance magnitudes for the two thermal conditions generally agreed more closely, although differences as great as 20 dB still existed at some frequencies. For equal $Q_1(nf_0)$, the difference between the impedance spectra of Figures 4 and 5 for corresponding thermal conditions is the insertion loss due to the muffler. Observe that the muffler insertion loss was quite different for the conditions I and II. For condition I, insertion losses of 3 to 50 dB are observed, while insertion losses of 5 to 35 dB resulted for condition II. Observe also that the insertion loss for each thermal condition was different at each harmonic.

To compare the stepped-tube condenser model to that used by previous investigators [1-3], this study was repeated with the condenser modeled as anechoic, i.e., as an infinitely long tube of uniform area. When the muffler was not included in the discharge system model, the resulting $Z_{1,11}$ spectrum was signifigantly different from that for either stepped-tube model, as Figure 4 indicates, with greater differences observed for thermal condition I in general, and at the lower frequencies for both thermal conditions. Figure 5 shows that when the muffler was included, the impedance spectrum for the anechoic condenser model generally agreed with those for both stepped-tube models. The muffler insertion loss with the anechoic condenser model was also different from that predicted with either of the stepped-tube models.

5. CONCLUDING REMARKS

An approximate acoustic transfer matrix model for condensers in vapor compression refrigeration systems has been developed. This work is a first attempt to account for the effects of thermal variables on the acoustical performance of refrigeration systems. Although a simple and mathematically tractable heat exhanger geometry was considered, the method proposed for constructing a stepped-tube acoustic model could be applied to real condensers with more complicated heat transfer. This method could also be applied to evaporators for analysis of suction pressure pulsations.

The example cases considered show that the acoustic behavior of the condenser is strongly influenced by system thermal conditions, particularly at the first few harmonics of f_0, which often dominate reciprocating compressor discharge pulsation spectra. The results indicate that the anechoic condenser model is probably not adequate for predicting low frequency discharge pulsations in systems without mufflers. At the higher frequencies or for systems having a muffler separating the condenser from the compressor, the anechoic condenser and both stepped-tube condenser models seem to give similar results. The muffler insertion loss spectrum was found to be different for all three condenser models. This suggests that muffler performance may be influenced by thermal conditions, and that the anechoic condenser model may not be adequate for predicting muffler performance.

ACKNOWLEDGEMENT

The authors gratefully acknowledge Copeland Corporation and Carrier Corporation for their financial support of this work.

REFERENCES

1. R. Singh and W. Soedel 1979 *Journal of Sound and Vibration* **63**, 125-143. Mathematical modeling of multicylinder compressor discharge interactions.

2. J. J. Nieter and R. Singh 1984 *Journal of Sound and Vibration* **97**, 475-488. A computer simulation of compressor tuning phenomena.

3. F. Scheideman, M. Schary, and R. Singh 1978 *Proceedings of Purdue Compressor Technology Conference*, 290-299. Thermodynamic and acoustic simulation of positive displacement refrigeration compressors.

4. M. L. Munjal 1987 *Acoustics of Ducts and Mufflers with Application to Exhaust and Ventilation System Design*. New York: Wiley.

5. M. L. Munjal and A. V. Sreenath 1973 *The Shock and Vibration Digest* **5**, 2-14. Analysis and design of exhaust mufflers-recent developments.

6. M. J. Crocker 1977 *Proceedings of NOISE-CON 77*, 331-358. Internal combustion engine exhaust muffling.

7. J. E. Farstad 1987 *M. Sc. Thesis, The Ohio State University*. Pressure pulsation phenomena in refrigeration discharge systems.

8. S. M. Zivi 1964 *American Society of Mechanical Engineers, Journal of Heat Transfer* **86**, 247-252. Estimation of steady-state void fraction by means of the principle of minimum entropy production.

9. S. N. Rschevkin 1963 *A Course of Lectures on the Theory of Sound*. New York: MacMillan.

10. E. I. DuPont de Nemours and Co. 1964 *Thermodynamic Properties of Freon-12 Refrigerant*. Wilmington: DuPont.

11. J. Baustin, M. Pate, and A. Bregles 1986 *ASHRAE Transactions* **92**, 55-73. Properties of oil-refrigerant liquid mixtures with application to oil concentration measurement: Part1-thermophysical and transport properties.

12. W. M. Rohsenow and J. P. Hartnett 1973 *Handbook of Heat Transfer*. New York: McGraw-Hill.

Table 1. Refrigeration system thermal conditions.

Condition Designation	Refrigerant Flow Rate kg/hr (lb/hr)	Suction Pressure kPa (psig)	Discharge Pressure kPa (psig)	Condenser Exit Temp. K (F)	Compressor Inlet Temp. K (F)	Cooling Water Flow Rate kg/hr (lb/hr)	Cooling Water Inlet Temp. K (F)
I	97.1 (214)	344.7 (50.0)	1723 (250)	316 (110)	289 (60)	214 (471)	289 (61)
II	111.6 (246)	344.7 (50.0)	1206 (175)	298 (77)	289 (60)	894 (1970)	289 (61)

Table 2. Stepped -tube condenser models for two different thermal conditions.

	Element length for each thermal condition, mm (in)										
Element Area mm^2 (in^2)	126.6 (0.196)	120.3 (0.187)	107.7 (0.167)	95.0 (0.147)	82.3 (0.128)	69.7 (0.108)	57.0 (0.088)	44.3 (0.069)	31.7 (0.049)	19.0 (0.029)	6.32 (0.010)
I	2540 (100)	2413 (95)	1778 (70)	1143 (45)	1016 (40)	762 (30)	762 (30)	635 (25)	508 (20)	508 (20)	254 (10)
II	2667 (105)	3048 (120)	1397 (55)	1016 (40)	508 (20)	381 (15)	381 (15)	254 (10)	254 (10)	127 (5)	127 (5)

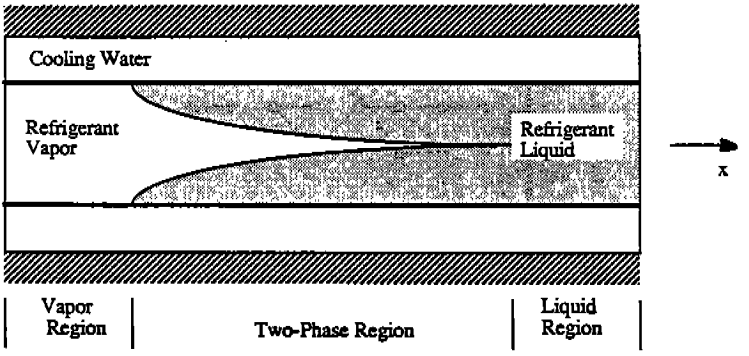

Figure 1. Water cooled, concentric tube heat exchanger.

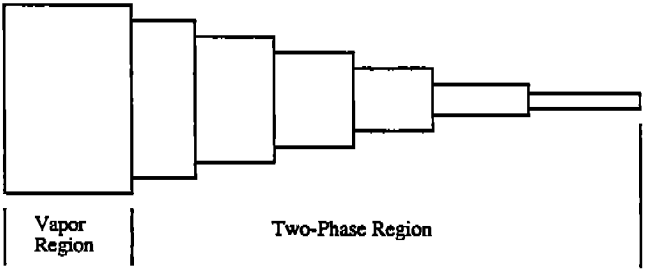

Figure 2. Stepped tube acoustic model for the condenser.

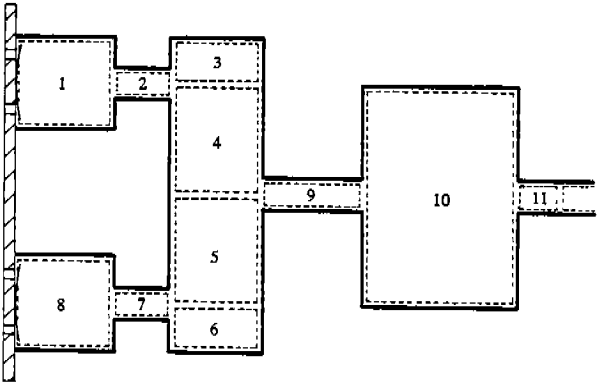

Figure 3. Compressor discharge system acoustic model.

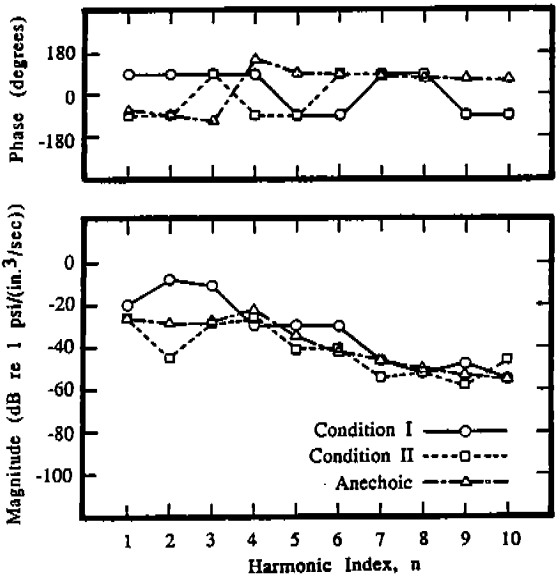

Figure 4. Valve chamber to discharge line acoustic impedance for systems without mufflers.

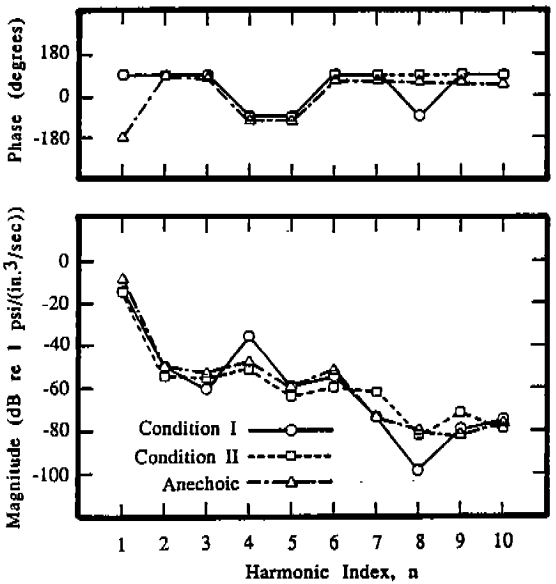

Figure 5. Valve chamber to discharge line acoustic impedance for systems with mufflers.